

## Recent results on doubly-polarised pion photoproduction and the GDH sum rule on the nucleon at MAMI

Susanna Costanza<sup>1,2,a</sup> for the A2 Collaboration

<sup>1</sup>*Dipartimento di Fisica, Università degli Studi di Pavia, I-27100 Pavia, Italy*

<sup>2</sup>*INFN, Sezione di Pavia, I-27100 Pavia, Italy*

**Abstract.** New measurements of the helicity dependence of the total inclusive photo-absorption cross section and of the partial cross sections for several reaction channels on the proton and on the neutron were carried out at MAMI (Mainz) in the energy region  $200 < E_\gamma < 1500$  MeV. The experiments were performed at the tagged photon beam facility of the MAMI accelerator in Mainz, using circularly and longitudinally polarised photons on longitudinally polarised proton, deuteron and  $^3\text{He}$  targets.

These new doubly-polarised pion-photoproduction data sets give new input to the partial wave analyses and allow to constrain the multipole solution of the different analyses; they also allow to study the double-polarisation observables G and E. Furthermore, the results obtained give information on the well-known Gerasimov-Drell-Hearn sum rule.

### 1 Introduction

In the past 50 years, the structure of the nucleus has been a central issue of nuclear and particle physics and the subject of intense research, both from the theoretical and experimental point of view. Of particular interest is the study of the excited states of the nucleon: as the excitation spectra of atoms reflect the properties of the electromagnetic interaction, the excited states of the nucleon are related to the fundamental properties of the strong interaction.

Since Quantum Chromodynamics (QCD) is non-perturbative at this energy scale, we have to rely on phenomenological quark models to interpret the experimental results. This approach has limited success, if one thinks about the “missing resonances” issue: at present, the experimental findings are quite in agreement with what models predict in the low mass region of the spectrum, but there is still a plethora of higher lying states predicted by theories and not yet observed.

From the experimental point of view, the reason for this mismatch can be due to data analysis relying mostly on pion scattering, that will therefore miss states that couple only weakly to  $\pi N$ : it may be that the higher lying states couple preferentially to decay channels involving heavier mesons or decay via intermediate excited states [1].

For a better understanding of the nucleon excitation spectra, the alternative is to use electromagnetic-induced reactions, like meson photoproduction: they allow to explore multiple meson production states, like  $\pi\pi$ ,  $\pi\eta$ , ... and access resonances that decay mainly via intermediate excited states (Fig. 1). In particular, photoproduction reactions of single pseudoscalar mesons allow to measure a set of 16

<sup>a</sup>e-mail: susanna.costanza@pv.infn.it

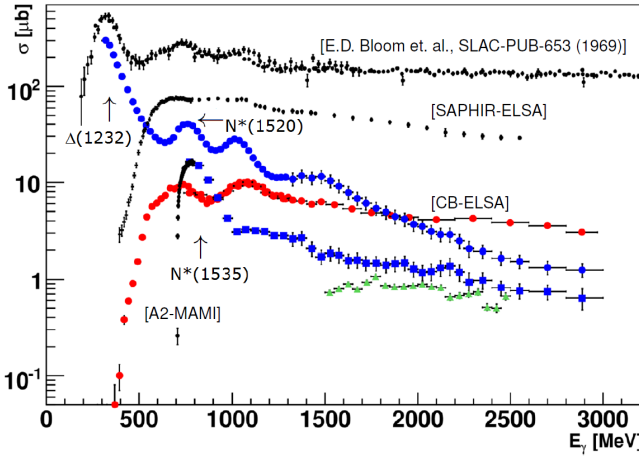


**Figure 1.** Cross section distributions for different reaction channels, showing the contributions of the different resonances:  $\gamma p \rightarrow X$  and  $\gamma p \rightarrow p\pi^-\pi^+$  (black),  $\gamma p \rightarrow p\pi^0\pi^0$  (red),  $\gamma p \rightarrow p\pi^0$  (blue circles),  $\gamma p \rightarrow p\eta$  (blue squares),  $\gamma p \rightarrow p\eta'$  (green triangles).

polarisation observables, for every fixed value of energy and angle ( $W, \theta$ ). In addition to the unpolarised cross section  $\sigma$ , there are 3 single polarisation observables and 12 double polarisation observables, grouped in beam-target, beam-recoil nucleon and target-recoil polarisation classes (Table 1). The measurement of 7 (8) properly chosen observables is necessary to yield a model-independent complete analysis [2, 3].

**Table 1.** Polarisation observables.

Photon polarisation		Target polarisation	Recoil nucleon polarisation	Target and recoil polarisation
		X Y $Z_{(beam)}$	$X'$ $Y'$ $Z'$	$X'$ $X'$ $Z'$ $Z'$ X Z X Z
unpolarised	$\sigma$	- T -	- P -	$T_{X'}$ $L_{X'}$ $T_{Z'}$ $L_{Z'}$
linear	$-\Sigma$	H (-P) -G	$O_{X'}$ (-T) $O_{Z'}$	$(-L_{Z'})$ $(T_{Z'})$ $(L_{X'})$ $(-T_{X'})$
circular	-	F - -E	$C_{X'}$ - $C_{Z'}$	- - - -

## 2 Double polarisation observables G and E

As described in Table 1, the polarisation observables G and E require the polarisation of both the photon beam and the target. In the following, the results obtained by the A2 Collaboration will be shown.

### 2.1 The experimental setup

The first experiment for the measurement of the double-polarisation observables E and G simultaneously using a longitudinally polarised electron beam in combination with a diamond radiation, thus resulting in an elliptically polarised photon beam, has been performed by the A2 Collaboration at the tagged photon facility of MAMI in Mainz (Germany).

The photon beam was produced via bremsstrahlung of an electron beam of 1557 MeV, provided by the

MAMI accelerator and polarised up to  $\sim 75\text{-}78\%$ . The photons were then tagged using the Glasgow-Mainz magnetic spectrometer with an energy resolution of  $\sim 2$  MeV.

For this experiment, a frozen-spin butanol ( $\text{C}_4\text{H}_9\text{OH}$ ) [4] target was used: the 2 cm long target cell was located in a  $^3\text{He}/^4\text{He}$  dilution refrigerator and the target nucleons were polarised via Dynamic Nuclear Polarisation (DNP) [5] to an initial polarisation degree up to 90%. During the data taking, a magnetic field of 0.68 T together with the 25 mK temperature provided by the dilution refrigerator ensured long relaxation times (up to 2000 h) before repolarisation was required. Since only the hydrogen nuclei of the butanol can be polarised, a carbon foam target was used in a dedicated beamtime to study background contributions from unpolarised carbon nuclei.

The target cell was placed inside the central detector system, devoted to the detection of the reaction products. It was composed by the Crystal Ball (CB) NaI spectrometer, a large solid angle, highly segmented photon and hadron spectrometer, and it was complemented by the Multi-Wire Proportional Chambers (MWPCs), used to discriminate between the charged and the neutral particles detected in CB. Precise energy information, as well as angle and particle identification in the azimuthal ( $\phi$ ) and polar ( $\theta$ ) angular regions from  $0^\circ$  to  $360^\circ$  and from  $21^\circ$  to  $159^\circ$ , respectively, are obtained by combining the information from these three detectors.

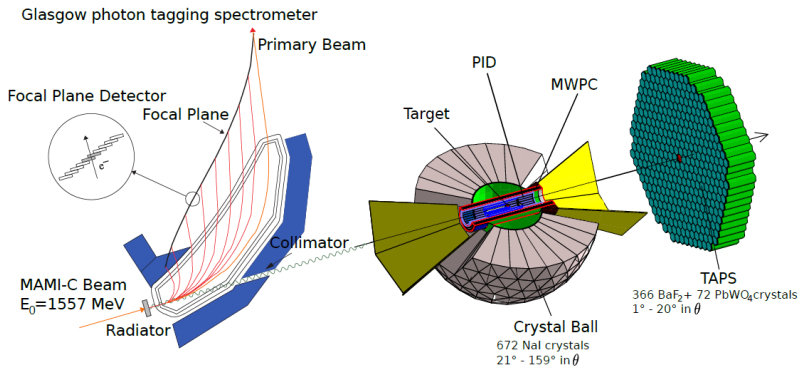


**Figure 2.** Schematic view of the A2 experimental setup.

## 2.2 The experimental results

The double polarisation observables  $E$  and  $G$  were calculated by using the differential cross section for pseudo-scalar meson photoproduction; in the case of elliptically polarised photons in combination with a longitudinally polarised target, it is given by:

$$\frac{d\sigma}{d\Omega}(\theta, \phi) = \frac{d\sigma}{d\Omega_0}(\theta) [1 - P_{lin}\Sigma \cos(2(\alpha - \phi)) - P_z(-P_{lin}G \sin(2(\alpha - \phi)) + P_{circ}E)]. \quad (1)$$

By integrating Eq. 1 over  $\phi$ , it is possible to extract the  $E$  observable:

$$N_B^{\left|_{\pm\alpha}^{\pm P_z}\right.}(\theta) = N_B(\theta) \cdot [1 - P_{circ}P_zE] \rightarrow E = \frac{\sigma^{1/2} - \sigma^{3/2}}{\sigma^{1/2} + \sigma^{3/2}} = \frac{N_B^{1/2} - N_B^{3/2}}{N_B^{1/2} + N_B^{3/2}} \cdot \frac{1}{d} \cdot \frac{1}{P_{circ}P_z}, \quad (2)$$

where  $N_B^{1/2}$  and  $N_B^{3/2}$  are the helicity-dependent count rates,  $d$  is the dilution factor and  $P_{circ}P_z$  the target and beam polarisation degrees. As the data were obtained with a butanol target, both the polarisable free protons in hydrogen nuclei and the unpolarised bound nucleons in carbon and oxygen

nuclei contribute to the count rates. This is taken into account by the dilution factor  $d$ , which specifies the amount of polarisable free protons in the data ( $d = N_{free}/(N_{free} + N_{bound})$ ). The factor  $d$  was determined during a dedicated data taking using a carbon foam target, by scaling the coplanarity distribution of the carbon data ( $N_C$ ) to the one of the butanol data ( $N_B$ ):  $d = 1 - s \cdot N_C/N_B$ , where  $s$  takes into account possible differences in acceptance, photon flux and target density during the carbon and butanol beamtimes.

Similarly, by integrating Eq. 1 over all possible helicity states, one can get the observable  $G$ :

$$N_B \Big|_{\pm\alpha}^{\pm P_z}(\theta, \phi) = N_B(\theta) \cdot [1 - P_{lin}\Sigma_B \cos(2(\alpha - \phi)) + dP_{lin}P_z G \sin(2(\alpha - \phi))]. \quad (3)$$

The double polarisation observables  $G$  and  $E$  were extracted from the data according to Eqs. 2 and 3 as a function of the beam energy  $E_\gamma$  for the entire angular range  $-1 \leq \cos\theta_\pi \leq 1$ . Preliminary results for the photoproduction reaction  $\vec{\gamma}\vec{p} \rightarrow p\pi^0$  are shown in Figs. 3 and 4. The results are compared to data from the CBELSA/TAPS collaboration ([6] for the  $G$  observable and [7] for  $E$ ) and to different partial wave analyses: for both the double polarisation observables there is a good agreement with the existing data and mostly with the different PWA models, especially with the BnGa2014-02 PWA solution.

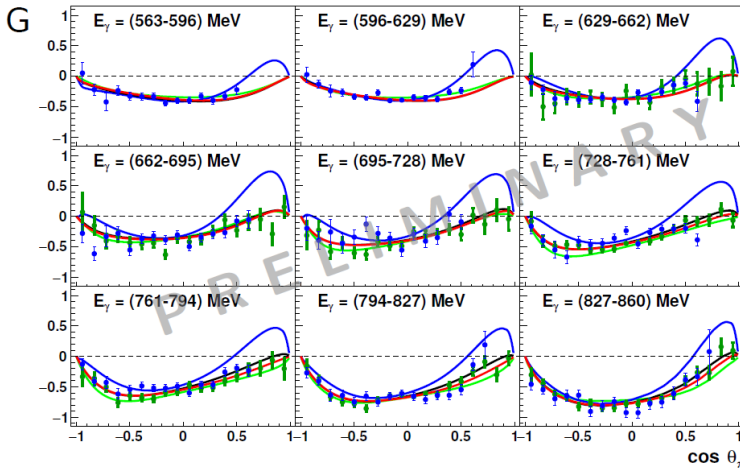


**Figure 3.** Results for  $G$  in  $\pi^0$ -photoproduction for selected energy bins, from 560 MeV to 860 MeV. The experimental results from A2 (blue circles) are compared to the CBELSA/TAPS data (green circles) [6], to PWA fits (BnGa\_2014\_02 [8], red line and BnGa\_2014\_01, black line) and PWA predictions from MAID2007 [9] (green line) and SAID-CM12 [10] (blue line).

### 3 The GDH sum rule

Sum rules are important tools to study the excited states of the nucleons, since they connect information from all energies to fundamental parameters of the interaction models of interest.

The Gerasimov-Drell-Hearn (GDH) sum rule [11, 12] relates the nucleon anomalous magnetic moment (AMM)  $\kappa$ , the spin  $S$  and the mass  $M$  of a nucleon to the integral over the weighted helicity difference of the total absorption cross section for circularly polarised photons on a longitudinally polarised nucleon target:

$$I_{GDH} = \int_{\nu_{th}}^{\infty} \frac{\sigma_p - \sigma_a}{\nu} d\nu = 4\pi^2 \kappa^2 \frac{e^2}{M^2} S, \quad (4)$$

where  $\nu$  is the photon energy, and  $\sigma_p$  and  $\sigma_a$  denote the total absorption cross section for parallel and antiparallel orientation of photon and particle spins, respectively. The lower limit of the integral,  $\nu_{th}$ ,

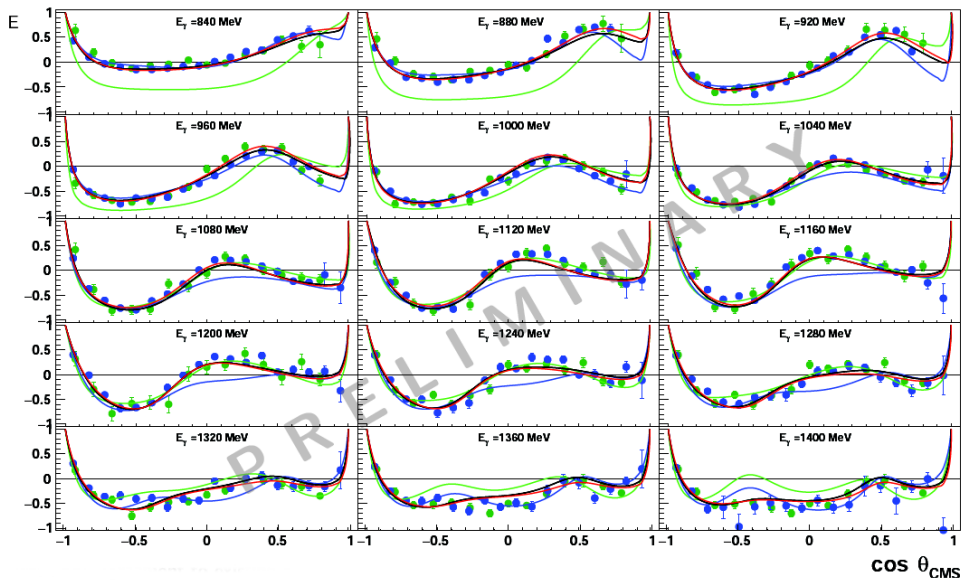


**Figure 4.** Results for  $E$  in  $\pi^0$ -photoproduction for selected energy bins from 840 MeV to 1400 MeV. The experimental results from A2 (blue circles) are compared to the CBELSA/TAPS data (green circles) [7], to PWA fits (BnGa\_2014\_02 [8], red line and BnGa\_2014\_01, black line) and PWA predictions from MAID2007 [9] (green line) and SAID-CM12 [10] (blue line).

corresponds to pion production and photodisintegration threshold for a nucleonic and nuclear target, respectively.

Since the GDH sum rule is derived from very general fundamental physical principles, like Lorentz invariance, the optical and the low energy theorems, the test of this relation represents a fundamental check of our knowledge of the  $\gamma$ -nucleon interaction, as well as of the physics of strongly interacting systems and of the existing photo-reaction models. In addition, through the helicity dependent  $N\pi$  channels, it is possible to access new observables and study the baryonic resonances, as well as test multipole models.

A comprehensive experimental program is carried out in Mainz since a few years, in order to give a better insight into the GDH sum rule on the proton and on the neutron, and to perform an accurate investigation of the properties of baryonic resonances.

### 3.1 The experimental setup

The experiments were carried out by the A2 Collaboration at the tagged photon facility of the MAMI accelerator in Mainz, using circularly polarised photons obtained by bremsstrahlung of longitudinally polarised electrons with an average polarisation of 75%.

For the studies on the proton, the frozen-spin butanol target data collected for the  $E$  and  $G$  double polarisation observables were used.

Polarised deuteron or high pressure  $^3\text{He}$  gas targets were used as polarised neutron sources. Longitudinally polarised deuterons were provided by a frozen spin target using deuterated butanol ( $\text{C}_4\text{OD}_{10}$ ): thanks to the use of a new doping material [13] it was possible to get a starting value of target polari-

sation up to 70%, with a relaxation time of  $\sim 200$  hours. Gaseous  $^3\text{He}$  was polarised via the method of metastability exchange optical pumping (MEOP [14]) and it was possible to obtain initial polarisation values up to 70%, with total relaxation time of  $\sim 20$  hours.

During the data taking, the photoemitted hadrons were registered by the large acceptance detector described in 2.1.

### 3.2 Results on the proton and deuteron

The preliminary results of the helicity dependence of the total inclusive cross section  $\Delta\sigma_{tot} = (\sigma_a - \sigma_p)$  on the proton and on the neutron are depicted in Fig. 5 (blue circles). They are compared to the results obtained by the GDH Collaboration [15, 16] (red circles) and are in good agreement within the errors. Fig. 6 shows the results for the partial channels  $\gamma p \rightarrow \pi^0 X$  and  $\gamma d \rightarrow \pi^0 X$ : also in these plots, the

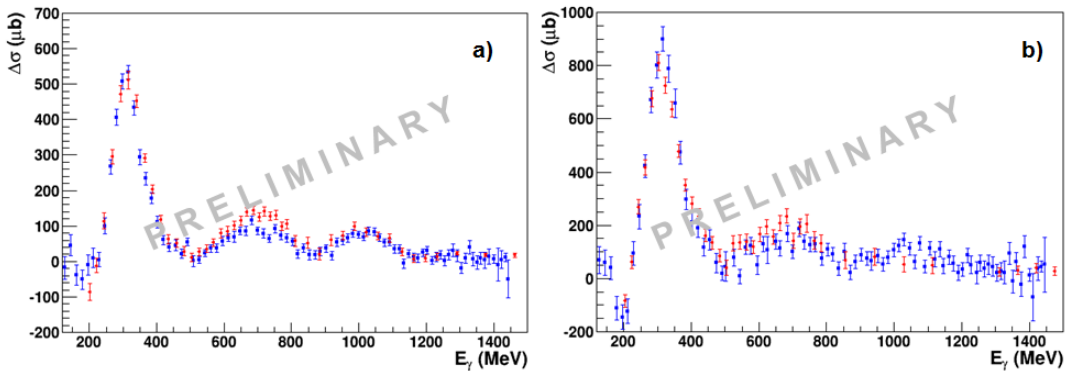


**Figure 5.** Helicity dependent total inclusive cross section for the  $\gamma p \rightarrow X$  (a) and  $\gamma d \rightarrow X$  channels (b). The A2 results (blue circles) are compared to the results from the GDH Collaboration (red circles) [15, 16].

A2 data (blue circles) are compared to the GDH Collaboration results, which are available only in the  $\Delta$ -resonance region, where the agreement is good. It is therefore clear from the plots that our recent results can provide a useful contribution in an energy region where no other data are available.

The A2 results are also compared to the predictions of the MAID multipole analysis: since the model is a free nucleon estimation, it does not take into account the nuclear effects in the deuteron case, where the discrepancy with the data is evident.

### 3.3 Results on $^3\text{He}$

In Figure 7, the unpolarised and helicity-dependent total cross sections for the partial channels  $\gamma^3\text{He} \rightarrow \pi^0 X$  and  $\gamma^3\text{He} \rightarrow \pi^\pm X$  are shown in the energy region  $200 < E_\gamma < 500$  MeV [17].

The data are compared to the prediction of the Fix-Arenhövel (FA) model (red line) and of a simple plane-wave impulse approximation (PWIA) model (blue line): the first model is an extension of the model on the deuteron [18]; in the second model, the cross sections are evaluated as an incoherent sum of quasi-free single nucleon contributions, determined using the MAID multipole analysis and the momentum distribution of the nucleons inside  $^3\text{He}$  as parametrised in [19]. The difference between the two models, i.e. the role of nuclear effects, results in damping and broadening the peak corresponding to the  $\Delta$  resonance excitation.

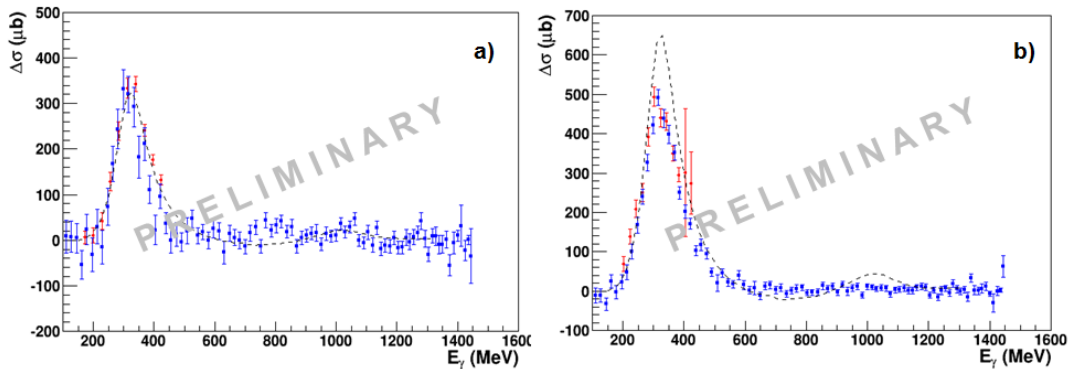


**Figure 6.** Helicity dependent total cross section for the semi-exclusive channels  $\gamma p \rightarrow \pi^0 X$  (a) and  $\gamma d \rightarrow \pi^0 X$  channels (b). The A2 results (blue circles) are compared to the results from the GDH Collaboration (red circles) [15, 16] and to the MAID model (dashed line).

In the unpolarised case, for the neutral partial channel the FA model is in good agreement with our data for  $E_\gamma \geq 250$  MeV, while it underestimated them at lower photon energies, where the coherent  $\gamma^3\text{He} \rightarrow \pi^0 \text{}^3\text{He}$  reactions is expected to play a dominant role. On the contrary, in the  $\pi^\pm X$  channel the FA model describes the measured cross section less well and for  $E_\gamma \geq 350$  MeV the PWIA model does better.

In the helicity dependent cross section case, as in the unpolarised case, the FA model describes the  $\gamma^3\text{He} \rightarrow \pi^0 X$  data at higher photon energies while it does not reproduce the shape of the experimental data of the charged partial channel. The PWIA model, instead, reproduces the data at higher  $E_\gamma$  values for both reaction reasonably well.

In order to better understand the origin of the observed discrepancies between the experimental models and the data, an analysis of both the unpolarised and polarised differential cross sections for the  $\gamma^3\text{He} \rightarrow \pi^0 X$  and  $\gamma^3\text{He} \rightarrow \pi^\pm X$  has been performed: the results can be found in [20].

## 4 Conclusions

Double polarised pion photoproduction experiments are a useful tool for the understanding of the nucleon excitation spectra.

The A2 Collaboration at MAMI has performed the first simultaneous measurement of the double polarisation observables E and G, by using a longitudinally polarised electron beam incident on a diamond radiator and a longitudinally polarised frozen-spin target. The preliminary results available up to  $E_\gamma = 1500$  MeV are in good agreement with existing data from the CBELSA/TAPS Collaboration and provide an original contribution in the  $\Delta(1232)$  resonance region.

The experimental data obtained from these experiments can be used also to study the Gerasimov-Drell-Hearn sum rule: the A2 Collaboration has carried out a comprehensive experimental program to study it on the proton, on the neutron and also on  $^3\text{He}$ . Preliminary results of the helicity dependent total inclusive  $\gamma p \rightarrow X$  and  $\gamma d \rightarrow X$  cross sections, and of the helicity dependent total cross sections for the semi-exclusive channels  $\gamma p \rightarrow \pi^0 X$  and  $\gamma d \rightarrow \pi^0 X$  are in reasonable agreement with the existing data from the GDH Collaboration. Furthermore, results on the helicity dependent  $\gamma^3\text{He} \rightarrow \pi X$  reactions have been shown up to  $E_\gamma = 500$  MeV. These unprecedented data of this kind have proved the feasibility of the use of polarised  $^3\text{He}$  gas target to check the GDH sum rule on the neutron.

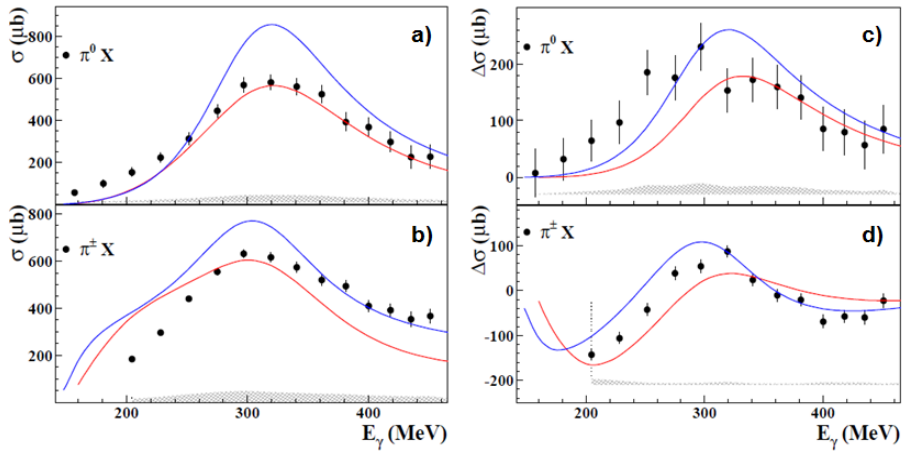


**Figure 7.** Unpolarised (left) and polarised (right) total cross section for  $\gamma^3\text{He} \rightarrow \pi^0 X$  (a and c) and  $\gamma^3\text{He} \rightarrow \pi^\pm X$  (b and d) channels. The error bars are statistical and the hatched bands show the systematic uncertainties. The measured cross sections are compared to the FA model (red line) and to our PWIA model (blue line).

## References

- [1] B. Krusche and S. Schadmand, arXiv:nucl-ex/0306023v1
- [2] I. S. Barker, A. Donnachie, J. K. Storrow, Nucl. Phys. **B95**, 347 (1975)
- [3] W.-T. Chiang and F. Tabakin, Phys. Rev. C **55**, 2054 (1997)
- [4] D. Goertz et al., Proceedings of PSTP205, PoS(PSTP2015)009 (2016)
- [5] D.G. Crabb and W. Meyer, Annu. Rev. Nucl. Part. Sci. **47**, 67 (1997)
- [6] A. Thiel et al., Phys. Rev. Lett. **109**, 102001 (2012)
- [7] M. Gottschall et al., Phys. Rev. Lett. **112**, 012003 (2014)
- [8] E. Gutz et al., Eur. Phys. J. A **50**, 74 (2014)
- [9] D. Drechsel, S.S. Kamalov and L. Tiator, Eur. Phys. J. A **34**, 69 (2007)
- [10] R.L. Workman, M.W. Paris, W.J. Briscoe, I.I. Strakovsky, Phys. Rev. C **86**, 015202 (2012)
- [11] S. B. Gerasimov, Sov. J. Nucl. Phys. **2**, 430 (1966)
- [12] S. D. Drell and A. C. Hearn, Phys. Rev. **96**, 1428 (1966)
- [13] S. Goertz et al., Nucl. Instr. Meth. A **526**, 43 (2004)
- [14] F. Colegrove et al., Phys. Rev. Lett. **132**, 2561 (1963)
- [15] J. Ahrens et al., Phys. Lett. B **672**, 328 (2009)
- [16] H. Dutz et al., Phys. Rev. Lett. **94**, 162001 (2005)
- [17] P. Aguar Bartolomè et al., Phys. Lett. B **723** (2013) 71-77
- [18] H. Arenhövel, A. Fix, Phys. Rev. C **72** (2005) 064004
- [19] R. Schiavilla, C. Pandharipande, Nucl. Phys. A **449** (1986) 219
- [20] S. Costanza et al., Eur. Phys. J. A (2014) **50**: 173